

Endothelin B receptor-mediated encephalopathic events  
in mouse sepsis model

(マウス敗血症モデルにおける、脳症とエンドセリン B レセプターの  
介在についての検討)

千葉大学大学院医学薬学府  
先端医学薬学専攻  
(主任：巽浩一郎教授)  
内藤 雄介

## **ABSTRACT**

*Aims:* We evaluated whether pathophysiological events in the brain in sepsis are mediated by ET-1/ET<sub>B</sub> receptor axis.

*Main methods:* We prepared raw fecal fluid from soft stool of mice. Mice were randomly divided into three groups: pre-PBS + raw fecal fluid group (Sepsis, easy stool method (ESM) group); pre-BQ788 + raw fecal fluid group (BQ group); and pre-BQ788 + PBS group (PBS group). According to each experimental condition, PBS or BQ788 was intravenously injected into mice prior to intraperitoneal administration of fecal fluid or PBS. All groups of mice were sacrificed at 8 h after administration, and then brain samples were prepared.

*Key findings:* In the ESM group, an increase of apoptotic neuroblasts was demonstrated in the subgranular zone of the hippocampal dentate gyrus, enhanced expression of c-FOS was observed in arginine-vasopressin-containing neurons in the hypothalamic paraventricular nucleus, and various cytokines involving TNF- $\alpha$  were upregulated in the brain, compared with those in the PBS group. In the region corresponding to their findings, the number of reactive microglia and vascular leakage were markedly increased. BQ788 inhibited the induction of c-FOS expression, neuroblast apoptosis, cytokine upregulation and reactive

microglia without affecting vascular leakage.

*Significance:* We demonstrated that BQ788 could protect the brain from the following sepsis-associated pathophysiological output: neural cell death, inflammatory response and the Hans Selye's environmental stress reaction.

## INTRODUCTION

Sepsis is a systemic inflammatory response that mainly results from bacterial infection (Bone et al. 1997; Levy et al. 2001). To date, severe sepsis and septic shock are still the most common cause of death in adult intensive care units, despite advances in critical care medicine (Moreno et al. 2008). It is therefore now more important to elucidate the mechanism of sepsis than to develop further effective treatment for it.

It has been reported that endothelin (ET)-1 is associated with severity of sepsis/endotoxemia (Pittet et al. 1991; Eakes et al. 1997). Likewise, nonselective ET receptor antagonist attenuated organ injury, and decreased mesenteric blood flow in endotoxemia/cecal ligation and puncture (CLP), which has been widely accepted as an animal model of sepsis (Erdem et al. 2007). In a neonatal sepsis model, blockade of ET<sub>A</sub> attenuated the inflammatory response and prolonged survival time (Goto et al. 2010). On the other hand, it is suggested that not ET<sub>A</sub> but ET<sub>B</sub> upregulated under polymicrobial septic condition plays a key role in alteration of hepatic hemodynamics (Kim et al. 2004; Eum et al. 2007). Likewise, nonselective ET<sub>A</sub>/ET<sub>B</sub> antagonist but not ET<sub>A</sub> antagonist markedly decreased the mortality rate of LPS-treated rats, and upregulation of both ET-1 and ET<sub>B</sub> in the heart of LPS-treated rats was observed, whereas ET<sub>A</sub> was markedly downregulated in

the heart, lung and liver of LPS-treated rats, suggesting a crucial role of ET<sub>B</sub> in the pathogenesis of sepsis (Ishimaru et al. 2001). These previous reports tempt us to consider the possibility that ET<sub>B</sub> rather than ET<sub>A</sub> might play the pathophysiological role in endotoxemia.

Sepsis-associated encephalopathy (SAE), a global cerebral dysfunction induced by the systemic response to inflammation and infection, is associated with increased morbidity and mortality (Ziaja. 2013). In patients with sepsis, patients with an acutely altered mental status due to sepsis had a higher mortality (49%) than patients with normal mental status (26%), indicating that SAE can lead to a 2-fold increase in the risk of death (Sprung et al. 1990). As a plausible scenario of SAE development, the following events are thought to occur sequentially: cerebral endothelial activation starts an inflammatory process by releasing inflammatory mediators or by leading inflammatory mediators into the parenchyma through the impaired blood-brain barrier (BBB); and inflammatory mediators affect cellular metabolism and activity of various types of cells resulting in pathologic abnormalities that range from alterations of neurotransmission to apoptosis (Sharshar et al. 2010). In the sequence of events, activated microglia is hypothesized to play a pivotal role in neuroinflammation leading to delirium (van Gool et al. 2010). However, the underlying

pathophysiology in SAE is still not fully understood. In addition, the correlation between SAE and ET/ETR signaling has never been demonstrated.

In the central nervous system (CNS), ET<sub>B</sub> is predominantly expressed in astrocytes and microglia (Ozawa et al. 1997; Ehninger and Kempermann 2008). Glial cells are strongly related to inflammatory response in the CNS via various functions such as antigen-presenting capacity, production of proinflammatory cytokines, and maintenance of the blood-brain barrier (Yuan et al. 2010). These findings suggest that the ET<sub>B</sub>-mediated signal could participate in inflammatory brain diseases, and that blockade of ET<sub>B</sub> may restore disorder of brain function induced by inflammation.

Here, we investigated whether BQ788, an ET<sub>B</sub>-selective antagonist, inhibits pathophysiological changes in the brain in response to sepsis, focusing on output of SAE, leakage of BBB, activation of glial cells, apoptosis of brain stem/progenitor cells and induction of cytokines in the brain.

## **MATERIALS AND METHODS**

### *Mice*

Male C57BL/6J mice were purchased from Clea Japan (Tokyo, Japan). We treated

8~10-week-old mice as subjects, and 10~12-week-old mice as stool donors. Animals were housed in the Animal Resource Facility at Chiba University under pathogen-free conditions and cared for according to the animal care guidelines of Chiba University. The studies were performed according to an animal protocol approved by the Committee of Animal Welfare of Chiba University.

#### *Induction of sepsis*

The intestine including the cecum from donor mice was excised, and soft stool was extracted in phosphate-buffered saline (PBS). The extracted stool was centrifuged at 500 g for 5 min, and the resulting supernatant was diluted with PBS to obtain turbidity of 0.15 at OD<sub>600</sub>. We have confirmed that intraperitoneal (i.p.) injection of 300 µl of stool fluid can induce sepsis in mice, with a pathological profile close to the common sepsis model, CLP (Dejager et al. 2011). Colony forming units of 300 µl of stool fluid were  $7 \times 10^5$ /24 h and  $1.7 \times 10^7$ /24 h under aerobic condition and anaerobic condition, respectively. By an analysis of genomic 16S rRNA sequences of each colony randomly picked up, the presence of *Bacillus*, *Bacteroides*, *Escherichia*, *Eubacterium*, *Lactococcus*, *Lactobacillus*, *Proteus* and *Parabacteroides* bacteria was confirmed, indicating that the stool fluid contains at least aerobic Gram-negative organisms leading to acute physiological features

of sepsis in human peritonitis (Parker and Watkins. 2001). Likewise, a comprehensive investigation of plasma cytokines/chemokines by western blot (WB) array indicated that stool fluid induces a cytokine storm in peripheral blood. Furthermore, all mice died within 24 h of stool fluid injection, indicating that our ESM induces a severe sepsis. (Naito et al. 2013; Manuscript in preparation). To evaluate the effect of BQ788 on the brain in sepsis, mice were divided into three groups: PBS group, intravenous (i.v.) injection of 500  $\mu$ l BQ788 (10  $\mu$ g/mouse) 15 min prior to i.p. injection of 300  $\mu$ l PBS; ESM group, i.v. injection of 500  $\mu$ l PBS 15 min prior to i.p. injection of 300  $\mu$ l stool fluid; and BQ group, i.v. injection of 500  $\mu$ l BQ788 (10  $\mu$ g/mouse) 15 min prior to i.p. injection of 300  $\mu$ l stool fluid. Mice were sacrificed after 8 h. We confirmed that an i.v. injection of BQ788 alone affects neither plasma levels of cytokines/chemokines nor brain histology under the resting state.

#### *Immunofluorescent study of brain sections*

After fixation followed by dehydration, the brains were frozen in Tissue Tek OCT compound (Sakura Finetek, Torrance, CA). Freshly cut brain sections (30  $\mu$ m) were subjected to reaction with rabbit anti-c-Fos antibody (Merck&Co., Inc., New Jersey), mouse anti-AVP antibody (Santa Cruz Biotech, Santa Cruz, CA), goat anti-doublecortin



(DCX) antibody (Santa Cruz Biotech), rabbit anti-cleaved/active caspase 3 antibody (Cell Signaling Technology, Framingham, MA), rabbit anti-ionized calcium binding adaptor molecule 1 (Iba1) antibody (WAKO, Tokyo, Japan) or mouse Cy3-conjugated anti-gial fibrillary acidic protein (GFAP) antibody (Sigma-Aldrich, St. Louis, MO). Sections reacted with anti-c-Fos, AVP, DCX, cleaved/active caspase 3 or Iba1 antibody were further stained with an appropriate fluorescein-conjugated second antibody. Nuclei were stained with 4'6-diamino-2-phenylindole (DAPI). In all experiments, coronal sections fitting to the same atlas images from each group (PBS, ESM and BQ; 6 mice/each group) were subjected to immunofluorescent study and observed under a fluorescence microscope (Axio Imager A2, Carl Zeiss, Oberkochen, Germany). In some experiments, fluorescence profiles were analyzed by an Image Gauge V4.21 (a densitometry software, FUJIFILM, Tokyo, Japan) to quantify the fluorescence intensity of Iba1-LI/Iba1<sup>+</sup> cell or GFAP-LI/GFAP<sup>+</sup> cell.

#### *Detection of ET-1-like immunoreactivity in the brain*

According to a previous report (Yoshimi et al. 1991), the fraction containing ET-1 was prepared from the brain at 8 h of PBS and ESM groups (3 mice/each group). After concentrating by a SEPAK C18 column (Sep-Pak® Waters Co., Milford, MA), the

resulting samples were lyophilized and dissolved in PBS. Then, the aliquots were subjected to an Endothelin-1 ELISA kit (Enzo Life Sciences, Inc., Farmingdale, NY) for detection of ET-1-like immunoreactivity (LI).

#### *Detection of cerebral vascular leakage*

The fluorescein-conjugated dextran (FITC-dextran, Sigma-Aldrich) of 10-kDa average molecular weight was used as the permeability tracer. The FITC-dextran solution (250  $\mu$ l of 10 mg /ml in PBS) was intravenously injected into mice from the caudal vein 15 min prior to the treatment of each group. At a designated time, mice were intracardially perfused with PBS, and the brains were dissected out. After fixation followed by dehydration, freshly cut brain sections (30  $\mu$ m) were observed under a fluorescence microscope. The resulting fluorescence profile of section was analyzed by an Image Gauge V4.21 to quantify the fluorescence intensity of FITC-dextran in each section.

#### *Expression of cytokines in the brain*

Mice at 8 h of each group were intracardially perfused with PBS, and the brains were dissected out. A 3 mm-thick coronal slice (-0.6 mm to bregma ~ +2.4 mm to bregma, covering the specific sites of brain where inflammation-associated pathophysiological features were observed) was prepared from each brain. After removing the cortex, the slice

was homogenized in the tissue lysis buffer (Tokuhara et al. 2010) and centrifuged at 9000 g for 15 min at 4°C. The resulting supernatant was used as a protein sample. The mixture (250 + 250 µg protein) of two samples from each group was subjected to Proteome Profiler Mouse Cytokine Array Kit (ARY 006, R&D systems, Inc., Minneapolis, MN). The array was performed twice according to the manufacturer's instructions. We confirmed the reproducibility of changes in expression of cytokines under each condition (PBS, ESM and BQ). Then, each cytokine signal was normalized to the positive internal control included in the array membrane by using an Image Gauge V4.21.

#### *Statistical analysis*

Data are expressed as mean ± S.E.M. Statistical analysis was conducted using Graphpad Prism Version 6 (GraphPad Software Inc., San Diego, CA). Statistical significance was determined by Student's *t* test or analysis of variance (ANOVA) followed by Tukey test, and *p* values < 0.05 were considered to be significant.

## **RESULTS**

### *Elucidation of initial encephalopathic events induced by ESM*

To elucidate whether ESM induces histopathological changes in the brain, we first investigated profiles of Iba1<sup>+</sup> microglia or GFAP<sup>+</sup> astrocyte in the brain. As shown in Fig. 1A, an immunoreactivity of Iba1 in the brain from the ESM group specifically increased in the dentate gyrus (DG) of the hippocampus, the thalamus and the hypothalamus compared with that from the PBS group. An increase in immunoreactivity of GFAP in the ESM group was observed in the corresponding area where Iba1-LI increased. Under these situations, ET-LI in the brain was significantly elevated by ESM (Fig. 1B). As the breakdown of BBB is one of typical events in SAE, a time-dependent vascular leakage was monitored by FITC-dextran. As shown in Fig. 1C, ESM induced the breakdown of BBB in the hippocampus within 1 h. Then, to address to whether ET-1/ ET<sub>B</sub> system is involved in the inflammation-associated changes in the brain, effect of BQ788 on ESM-induced pathophysiological changes in the specific sites was elucidated. A single i.v. injection of BQ788 was employed in the present study because the delivery of BQ788 to the brain parenchyma through the impaired BBB was expected (Fig. 1C). Likewise, it has been demonstrated that a single i.v. injection of BQ788 could exert its inhibitory effect at least for 5 h (Piechota-Polańczyk and Gorąca. 2012).

*ESM-induced pathophysiological changes in the DG*

As shown in Fig. 2A, ESM markedly induced both Iba1- and GFAP-LI in the hilus of the hippocampal DG compared with the case of the PBS group. Administration of BQ788 suppressed the ESM-induced Iba1- and GFAP-LI. Quantitative analyses showed that the number and the fluorescent intensity/cell of Iba1<sup>+</sup> cells and GFAP<sup>+</sup> cells were significantly increased by ESM. These parameters were significantly BQ788 treatment-sensitive (Fig. 2B & C). In such situations, active caspase 3<sup>+</sup>DCX<sup>+</sup> cells were typically observed in the subgranular zone (SGZ) of the hippocampal DG in the ESM group but not the PBS group, which was inhibited by BQ788 treatment (Fig. 2D). Changes in the number of active caspase 3<sup>+</sup>DCX<sup>+</sup> cells in the three groups are shown in Fig. 2E. On the other hand, the intensity of FITC-dextran in the hippocampus in the ESM group was markedly increased compared with that in the PBS group, which was not suppressed by BQ788 treatment (Fig. 2F).

*ESM-activated neuroendocrine cells in the paraventricular nucleus of the hypothalamus*

Typical profiles of c-FOS-LI observed in the paraventricular nucleus (PVN) of the hypothalamus in three groups were shown in Fig. 3A. The marked induction of c-FOS by ESM was significantly inhibited by BQ788 treatment (Fig. 3B). Most of c-FOS-LI induced by ESM were overlapped with AVP-LI in the PVN of the hypothalamus (Fig. 3C). In the

corresponding areas, the number of Iba1<sup>+</sup> and GFAP<sup>+</sup> cells was increased by ESM, which was sensitive to BQ788 treatment (Fig. 3D). BQ788 did not affect ESM-induced impairment of the BBB, the same as the case for the hippocampus (Fig. 3E).

#### *ESM-induced expression of cytokines in the brain*

To elucidate the relationships between the inflammation-associated pathophysiological output and inflammatory mediators, WB array analysis of cytokines in the specific sites of the brain was performed. Typical changes in expression of cytokines in three groups were shown in Fig. 4A, ESM obviously upregulated the expression of various cytokines, which was mostly sensitive to BQ788 treatment. A densitometric analysis of two experiments revealed that expression of 13 proteins exhibiting over 2-fold induction by ESM was reduced more than 30% by BQ788 treatment. Those 13 proteins' names were indicated with the correct location in the membrane map (Fig. 4A), and each signal expressed as an average intensity of two experiments was shown in Fig. 4B.

## **DISCUSSION**

Sepsis is associated with marked brain inflammation, and the resulting brain dysfunction including neuronal apoptosis and neuroendocrine system damage affects sepsis-induced

organ dysfunction in a positive feedback manner (Sharshar et al. 2005). However, sepsis-associated apoptosis of brainstem/progenitor cells has not been clarified. Likewise, the correlation between the neuroendocrine cells-mediated hypothalamic-pituitary-adrenal (HPA) axis, a part of Hans Selye's environmental stress reaction, and sepsis remains to be elucidated. Furthermore, the involvement of the ET<sub>B</sub>-mediated signal in these sepsis-associated events has never been investigated. In the present study, we clearly showed that sepsis-associated encephalopathic events such as an increased number of reactive microglia and induction of various proinflammatory mediators could be regulated by ET-1/ET<sub>B</sub> axis in our ESM model mice. In particular, among the ESM-induced cytokines sensitive to BQ788 (Fig. 4B), TNF- $\alpha$  in concert with activated microglia plays a crucial role in the development of brain dysfunction after systemic infection (van Gool et al. 2010; Clark et al. 2010). In addition, we also found that ESM increased the number of active caspase 3<sup>+</sup>DCX<sup>+</sup> cells in the SGZ and c-FOS<sup>+</sup>AVP<sup>+</sup> cells in the hypothalamic PVN in the areas where an increase in both reactive microglia and astrocytes were observed. Furthermore, those events were significantly suppressed by BQ788.

The SGZ as well as subventricular zone (SVZ) is recognized as the major source of new neurons in the adult brain (Burtrum and Silverstein 1994). A sepsis-induced increase of

neurogenesis in the SVZ but not SGZ has been shown (Bakirci et al. 2011). This finding suggests that sepsis may not affect either apoptosis or neurogenesis in the SGZ, considering the context of apoptosis and neurogenesis in the adult brain (Chambers et al. 2004). In our sepsis model, however, typical inflammation-associated pathophysiological features were observed in the hippocampal DG. Then, active caspase 3<sup>+</sup>DCX<sup>+</sup> cells in the SGZ were evaluated. Caspase 3, which is often activated in the apoptotic pathway, is a reliable marker for apoptotic cells (Maurya et al. 2013). DCX is a microtubule-associated protein expressed by neuronal precursor cells and immature neurons in embryonic and adult cortical structures, indicating that DCX is a marker for neuroblasts (Gleeson et al. 1998). Hence, the changes in number of active caspase 3<sup>+</sup>DCX<sup>+</sup> cells in three groups (PBS, ESM and BQ) suggest that the ET<sub>B</sub> signal mediates sepsis-induced neural progenitor apoptosis in the SGZ. Apoptotic mediators for neural stem or progenitor cells in the hippocampus under pathophysiological conditions remain to be elucidated. It has reported that LPS-induced apoptosis in hippocampus-derived neural stem cells could be protected by imipramine, a tricyclic antidepressant drug, through upregulation of brain-derived neurotrophic factor (BDNF) (Peng et al. 2008). Likewise, the administration of imipramine to maternal deprivation stress model rats significantly suppressed the levels of TNF- $\alpha$



having a counter effect on BDNF in the serum and cerebrospinal fluid of rats (Réus et al. 2013). In line with these findings, TNF- $\alpha$  may be a prominent candidate for the neural progenitor apoptosis in the SGZ.

The HPA axis is activated during bacterial and viral infections (Webster and Sternberg 2004). Expression of c-FOS is often used as a marker of neuronal cell activation (Kovács 1998). Our finding that ESM-induced c-FOS expression was mostly overlapped with AVP<sup>+</sup> cells in the hypothalamic PVN strongly suggest the ESM-induced activation of neuroendocrine cells (Harbuz. 2002). The relationships between cytokines and HPA axis activation are well defined. In particular, IL-1 $\alpha/\beta$  leads to a potent and prolong activation of HPA axis, and TNF- $\alpha$  also plays an activator for HPA axis (Dunn. 2000). The ESM-induced IL-1 $\alpha$  and TNF- $\alpha$  expression sensitive to BQ788 suggest that the ET-1/ET<sub>B</sub> system-upregulated IL-1 $\alpha$  and TNF- $\alpha$  might affect HPA axis (Figs. 3 & 4B).

Monitoring BBB function by FITC-dextran showed that the cerebral vascular leakage was induced at least from 1h to 8 h after ESM application (Figs. 1C, 2F & 3E). The ESM-induced BBB breakdown was observed in the corresponding areas where the inflammation-associated pathophysiological output. However, BQ788 can block neural progenitor cell death and HPA axis activation associated with inflammatory changes in the

brain parenchyma in response to sepsis without affecting sepsis-induced impairment of the BBB. Previous report has clearly demonstrated that not ET<sub>A</sub> but ET<sub>B</sub> on endothelial cells plays a crucial role in the impairment of BBB function in concert with endogenous ET-1 (Reijerkerk et al. 2012). The BQ788-insensitive ESM-induced BBB breakdown in the present study may be explained by the finding that a high concentration of BQ788 is needed to express its inhibitory effect on BBB damage compared with the case of ET<sub>B</sub> shRNA (Reijerkerk et al. 2012) or by the possibility that ESM-induced insult in BBB may be far beyond the effect of BQ788. In any case, our finding that sepsis-associated various proinflammatory mediators in the brain was clearly sensitive to BQ788 regardless of the state of BBB suggest that ET-1/ET<sub>B</sub>-mediated CNS inflammation might be independent of systemic cytokines. This notion is supported by a previous report that TLR4 function in CNS-resident cells, independent of systemic cytokine effects, is required for sustained CNS-specific inflammation during endotoxemia (Chakravarty and Herkenham. 2005).

Under our current experimental condition of ESM, treatment of mice in sepsis with BQ788 could not increase the survival rate of mice. As a next step, to evaluate the possibility that BQ788 is used for treatment of sepsis, an electroencephalographic study and a survival rate analysis are needed under a moderate condition controlling the insult intensity of ESM.

## **CONCLUSION**

We newly demonstrated that ET<sub>B</sub>-mediated signaling participates in pathophysiological features of SAE.

## **Conflict of Interest Statement**

The authors declare that there is no conflict of interest.

## **Acknowledgement**

This work was supported in part by Grants-in-Aid for Scientific Research ((B), 24390137 to Y.K.) and for Challenging Exploratory Research (25670256 to Y.K.), and by the Takeda Science Foundation for Visionary Research (to Y.K.). We thank Dr. Wendy Gray for editing our manuscript.

## REFERENCES

- [1] Bone RC, Grodzin CJ, Balk RA. Sepsis: a new hypothesis for pathogenesis of the disease process. *Chest*. 1997; 112:235-43.
  
- [2] Levy MM, Fink MP, Marshall JC, Abraham E, Angus D, Cook D, et al. 2001 SCCM/ESICM/ACCP/ATS/SIS International Sepsis Definitions Conference. *Crit Care Med*. 2003; 31:1250-6.
  
- [3] Moreno RP, Metnitz B, Adler L, Hoechtl A, Bauer P, Metnitz PG. Sepsis mortality prediction based on predisposition, infection and response. *Intensive Care Med*. 2008; 34:496-504.
  
- [4] Pittet JF, Morel DR, Hemsén A, Gunning K, Lacroix JS, Suter PM, et al. Elevated plasma endothelin-1 concentrations are associated with the severity of illness in patients with sepsis. *Ann Surg*. 1991; 213:261-4.
  
- [5] Eakes AT, Howard KM, Miller JE, Olson MS. Endothelin-1 production by hepatic endothelial cells: characterization and augmentation by endotoxin exposure. *Am J Physiol*. 1997; 272:G605-11.

- [6] Erdem A, Sevgili AM, Akbiyik F, Atilla P, Cakar N, Balkanci ZD, et al. Tezosentan attenuates organ injury and mesenteric blood flow decrease in endotoxemia and cecal ligation and puncture. *J Surg Res.* 2007; 141:211-9.
- [7] Goto T, Hussein MH, Kato S, Daoud GAH, Kato T, Kakita H, et al. Endothelin receptor antagonist attenuates inflammatory response and prolongs the survival time in a neonatal sepsis model. *Intensive Care Med.* 2010; 36:2132-9.
- [8] Kim JY, Lee SM. Effect of ascorbic acid on hepatic vasoregulatory gene expression during polymicrobial sepsis. *Life Sci.* 2004; 75:2015–26.
- [9] Eum HA, Park SW, Lee SM. Role of nitric oxide in the expression of hepatic vascular stress genes in response to sepsis. *Nitric Oxide.* 2007; 17:126–33
- [10] Ishimaru S, Shichiri M, Mineshita S, Hirata Y. Role of endothelin-1/endothelin receptor system in endotoxic shock rats. *Hypertens Res.* 2001; 24:119-26.
- [11] Ziaja M. Septic encephalopathy. *Curr Neurol Neurosci Rep.* 2013; 13:383
- [12] Sprung CL, Peduzzi PN, Shantney CH, Schein RM, Wilson MF, Sheagren JN, et al. Impact of encephalopathy on mortality in the sepsis syndrome. *The Veterans*

Administration Systemic Sepsis Cooperative Study Group. Crit Care Med. 1990; 18:801-6.

[13] Sharshar T, Polito A, Checinski A, Stevens RD, Septic-associated encephalopathy - everything starts at a microlevel. Crit Care. 2010; 14:199.

[14] van Gool WA, van de Beek, Eikelenboom P. Systemic infection and delirium: when cytokines and acetylcholine collide. Lancet. 2010; 375:773–75.

[15] Ozawa F, Kasuya Y, Hama H, Asada S, Inada T, Goto K. Microtubule dynamics regulates the level of endothelin-B receptor in rat cultured astrocytes. J Neurochem. 1997; 69:562-9.

[16] Ehninger D, Kempermann G. Neurogenesis in the adult hippocampus. Cell Tissue Res. 2008; 331:243-50.

[17] Yuan, TM, Sun Y, Zhan CY, Yu HM. Intrauterine infection/inflammation and perinatal brain damage: Role of glial cells and Toll-like receptor signaling. J Neuroimmunol. 2010; 229:16-25.

- [18] Dejager L, Pinheiro I, Dejonckheere E, Libert C. Cecal ligation and puncture: the gold standard model for polymicrobial sepsis? *Trends Microbiol.* 2011; 19:198-208.
- [19] Parker SJ, Watkins PE. Experimental models of Gram-negative sepsis. *Br J Surg.* 2001; 88:22-30.
- [20] Naito Y, Tanaka K, Matsunaga H, Nagano K, Ishida J, Fukamizu A, et al. Consideration about a new mouse model of sepsis. *J Pharmacol Sci.* 2013; 121 (Suppl. 1): 105P.
- [21] Yoshimi H, Kawanno Y, Akabane S, Ashida T, Yoshida K, Kinoshita O, et al. Immunoreactive endothelin-1 contents in brain regions deom spontaneously hypertensive rats. *J Cardiovasc Pharmacol.* 1991; 17 (Suppl. 7):S417-9.
- [22] Tokuhara N, Namiki K, Uesugi M, Miyamoto C, Ohgoh M, Ido K, et al. N-type calcium channel in the pathogenesis of experimental autoimmune encephalomyelitis. *J Biol Chem.* 2010; 285:33294-306.

- [23] Piechota-Polańczyk A and Gorąca A. Influence of specific endothelin-1 receptor blockers on hemodynamic parameters and antioxidant status of plasma in LPS-induced endotoxemia. *Pharmacol Reports*. 2012; 64:1134-41.
- [24] Sharshar T, Hopkinson NS, Orlikowski D, Annane D. Science review: The brain in sepsis—culprit and victim. *Crit Care*. 2005; 9:37-44.
- [25] Clark IA, Alleva LM, Vissel B. The roles of TNF in brain dysfunction and disease. *Pharmacol Ther*. 2010; 128:519-48.
- [26] Burtrum D, Silverstein FS. Hypoxic-ischemic brain injury stimulates glial fibrillary acidic protein mRNA and protein expression in neonatal rats. *Exp Neurol*. 1994; 126:112-8.
- [27] Bakirci S, Kafa IM, Uysal M, Kurt MA. Increased adult neurogenesis in the subventricular zone in a rat model of sepsis. *Neurosci Lett*. 2011; 497:27-31.
- [28] Chambers RA, Potenza MN, Hoffman RE, Miranker W. Simulated apoptosis/neurogenesis regulates learning and memory capabilities of adaptive neural networks, *Neuropsychopharmacology*. 2004; 29:747-58.



- [29] Maurya SK, Tewari M, Sharma B, Shukla HS. Expression of procaspase 3 and activated caspase 3 and its relevance in hormone-responsive gallbladder carcinoma chemotherapy. *Korean J Intern Med.* 2013; 28:573-8.
- [30] Gleeson JG, Allen KM, Fox JW, Lamperti ED, Berkovic S, Scheffer I, et al. Doublecortin, a brain-specific gene mutated in human X-linked lissencephaly and double cortex syndrome, encodes a putative signaling protein. *Cell.* 1998; 92: 63-72.
- [31] Peng CH, Chiou SH, Chen SJ, Chou YC, Ku HH, Cheng CK. Neuroprotection by Imipramine against lipopolysaccharide-induced apoptosis in hippocampus-derived neural stem cells mediated by activation of BDNF and the MAPK pathway. *Eur Neuropsychopharmacol.* 2008; 18:128–40.
- [32] Réus GZ, dos Santos MAB, Abelaira HM, Ribeiro KF, Petronilho F, Vuolo F. Imipramine reverses alterations in cytokines and BDNF levels induced by maternal deprivation in adult rats. *Behav Brain Res.* 2013; 242:40-6.
- [33] Webster JI, Sternberg EM. Role of the hypothalamic-pituitary-adrenal axis, glucocorticoids and glucocorticoid receptors in toxic sequelae of exposure to bacterial and viral products. *J Endocrinol.* 2004; 181:207-21.

- [34] Kovács KJ. c-Fos as a transcription factor: a stressful (re)view from a functional map. *Neurochem Int.* 1998; 33:287-97.
- [35] Harbuz M. Neuroendocrine function and chronic inflammatory stress. *Exp Physiol.* 2002; 87:519-25.
- [36] Dunn AJ. Cytokine activation of the HPA axis. *Ann N Y Acad Sci.* 2000; 917:608-17.
- [37] Reijerkerk A, Lakeman KAM, Drexhage JAR, van het Hof B, van Wijck Y, van der Pol SMA. Brain endothelial barrier passage by monocyte is controlled by the endothelin system. *J Neurochem.* 2012; 121:730-7.
- [38] Chakravarty S, Herkenham M. Toll-Like Receptor 4 on Nonhematopoietic Cells Sustains CNS Inflammation during Endotoxemia, Independent of Systemic Cytokines. *J Neurosci.* 2005; 25:1788–96.

Fig.1

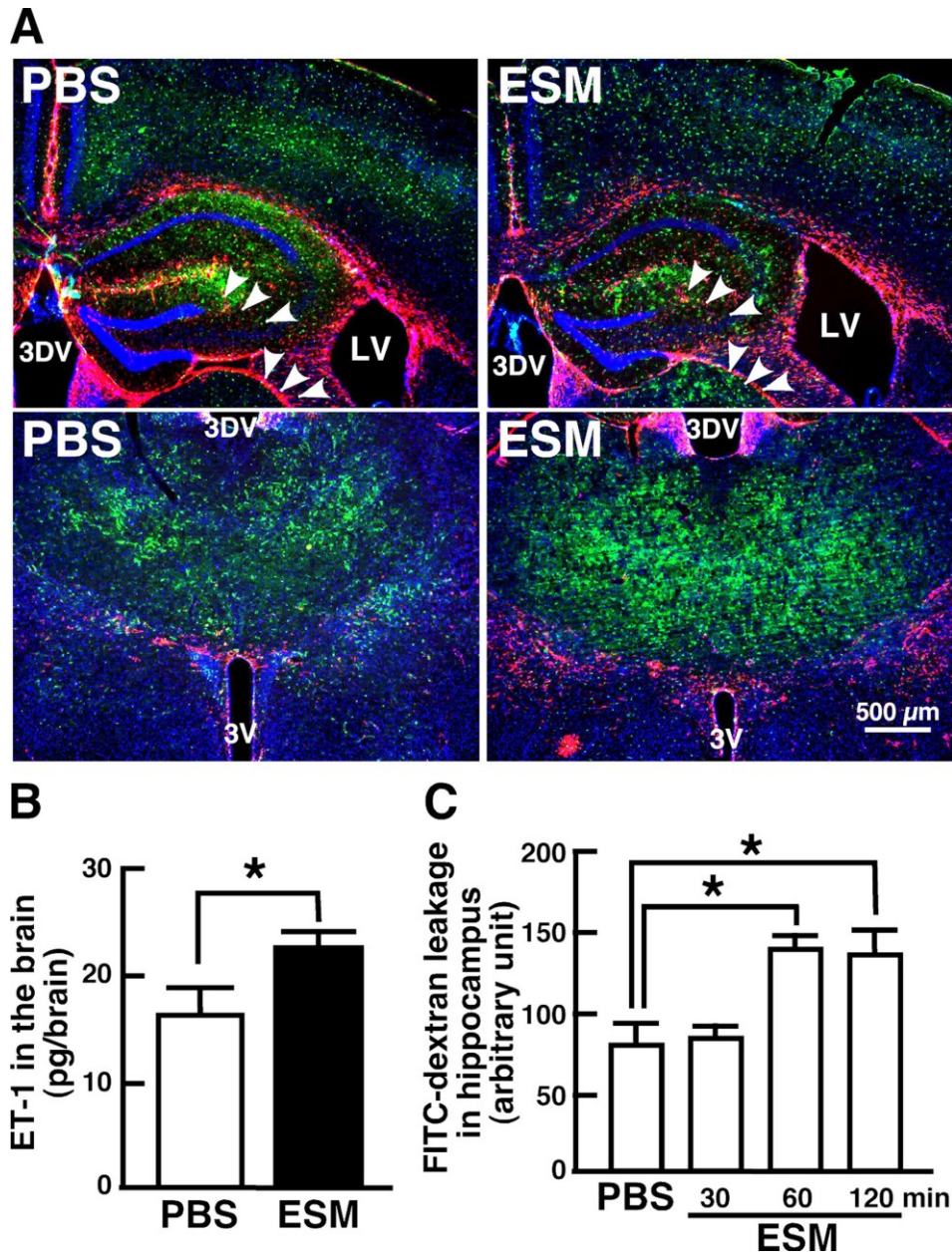


Fig.2

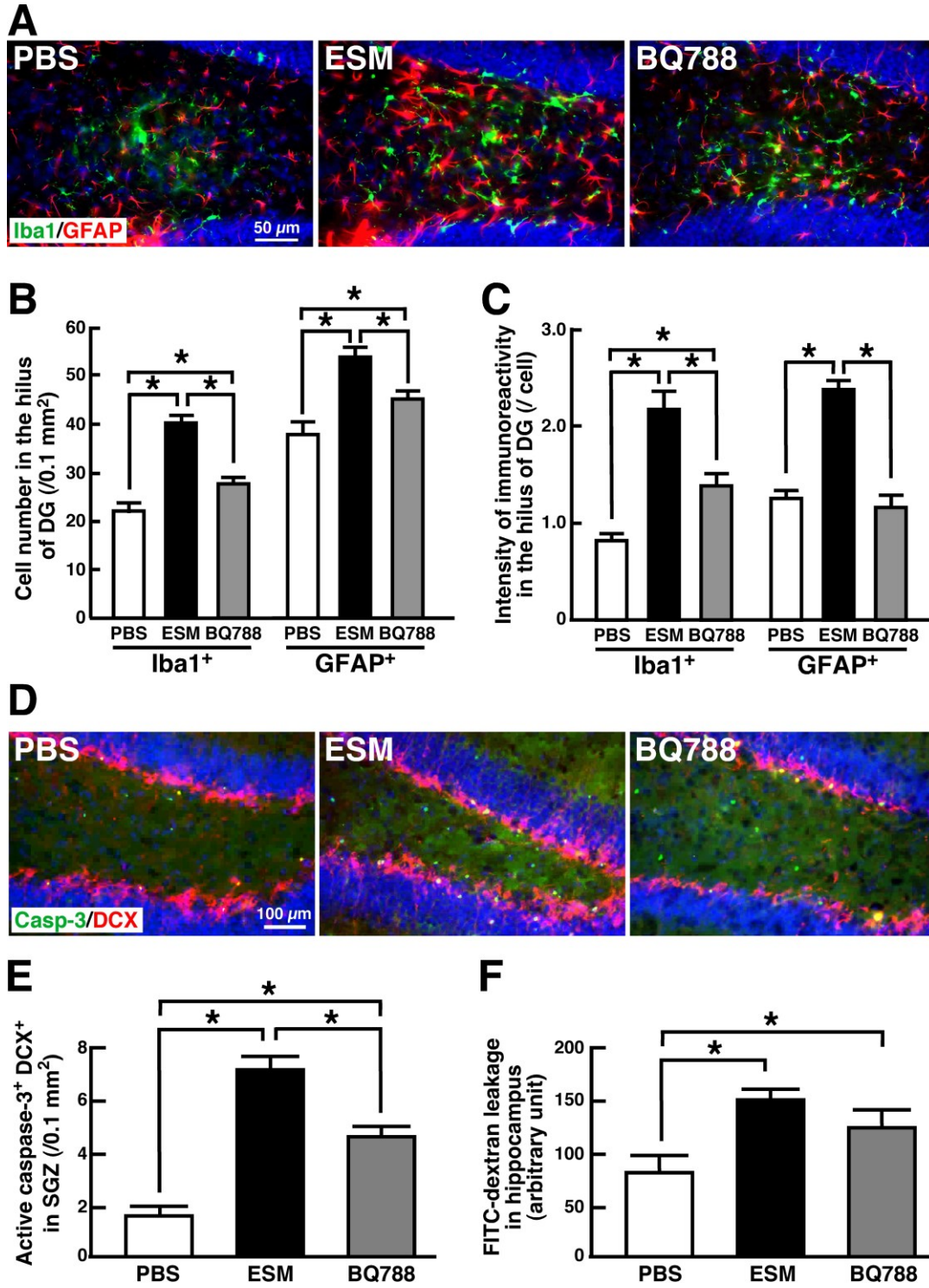


Fig.3

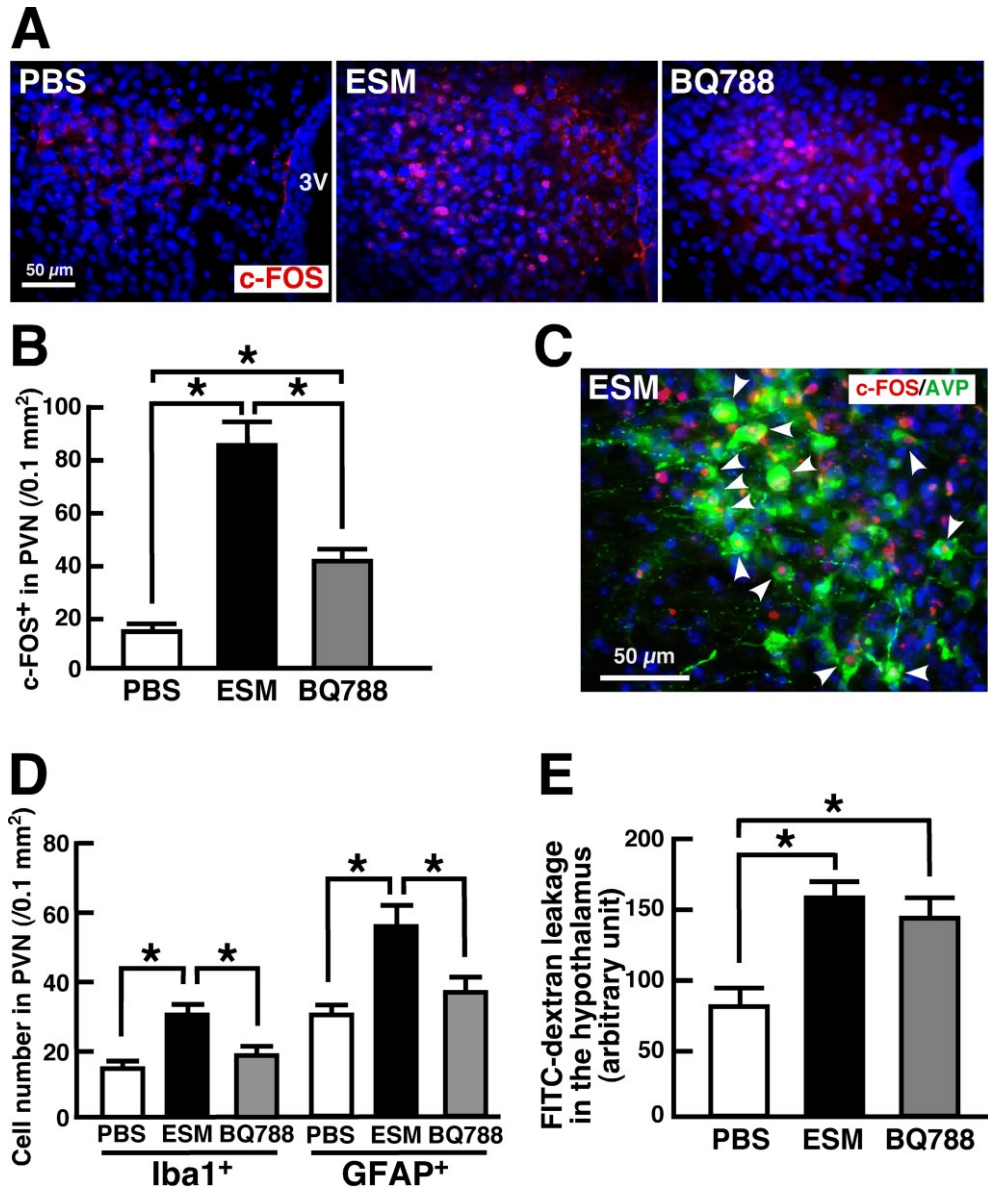
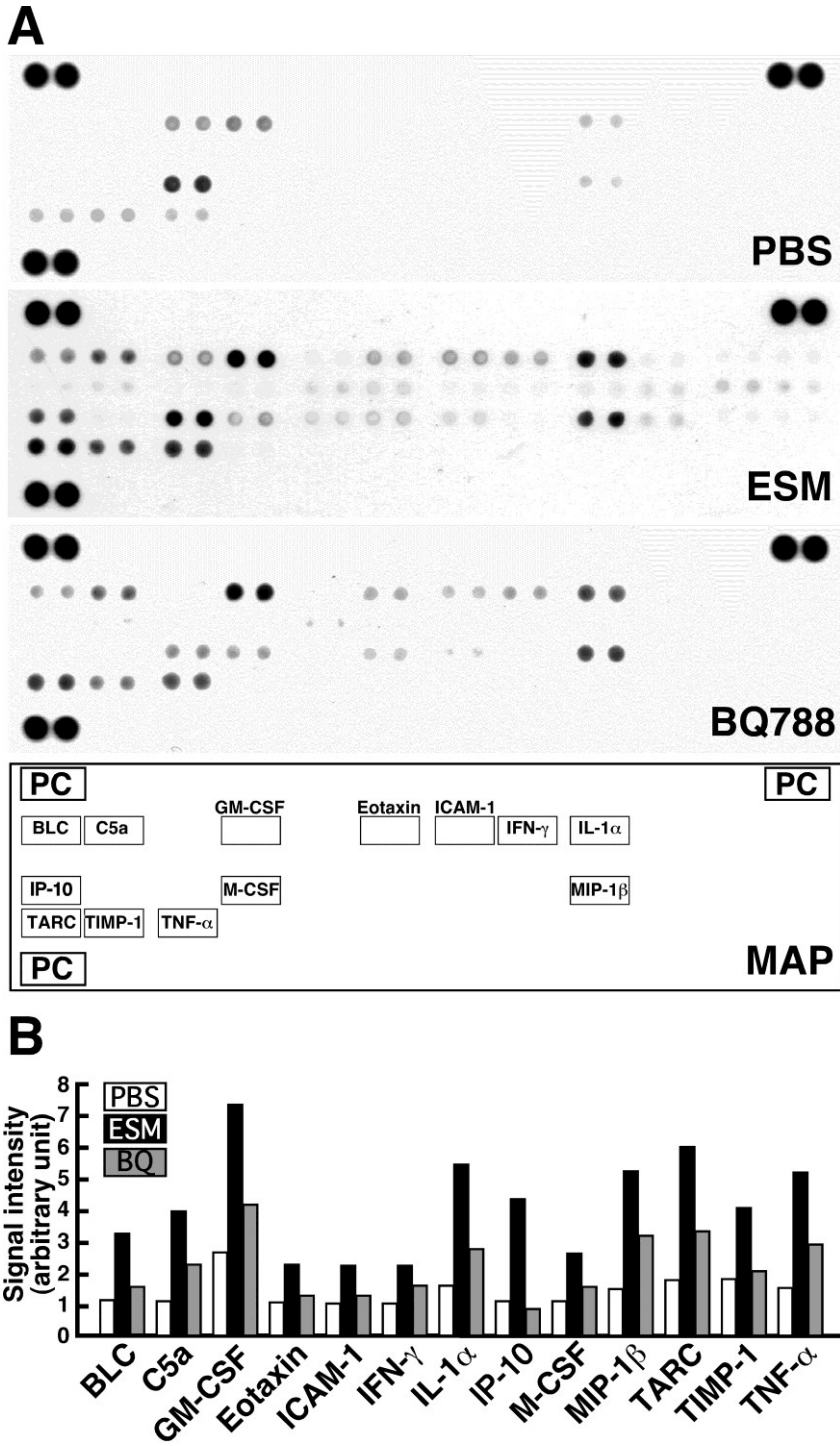


Fig.4



## FIGURE LEGENDS

**Figure 1** ESM-induced pathophysiological output in the brain. **A)** Iba1-LI and GFAP-LI in the PBS and ESM groups. Coronal sections fitting to the same atlas images from each group (8 h after treatment) were immunostained with anti-Iba1 (green) and anti-GFAP (red). All sections were stained with DAPI (blue). Arrow heads indicate matching areas between two groups. Similar results were obtained in independent experiments (n=6). **B)** ESM induces ET-1 expression in the brain. The brain from each group (8 h after treatment) was subjected to ET-1 extraction and concentration followed by EIA. Data are shown as mean with S.E.M (n=3). \* $P < 0.05$  (Student's *t* test). **C)** ESM induces cerebral vascular leakage. Hippocampi of coronal sections fitting to the same atlas images from the FITC-dextran-loaded brains of each group (indicated time after treatment) were observed under a fluorescence microscope. The fluorescence intensity of FITC was analyzed by a densitometer. Data are shown as mean with S.E.M (n=4). \* $P < 0.05$  (ANOVA followed by Tukey test). LV, lateral ventricle; D3V, dorsal third ventricle; 3V, third ventricle.

**Figure 2** ESM-induced pathophysiological output in the hippocampal DG. **A)** Typical profile of Iba1<sup>+</sup> and GFAP<sup>+</sup> cells in the DG in three groups (PBS, ESM and BQ788).

Coronal sections fitting to the same atlas images from each group (8 h after treatment) were immunostained with anti-Iba1 (green) and anti-GFAP (red). All sections were stained with DAPI (blue). **B)** The number of cells expressing Iba1 or GFAP in the hilus of the DG in three group. Data are shown as mean with S.E.M (n=6). \* $P < 0.05$  (ANOVA followed by Tukey test). **C)** The intensity of Iba1-LI/Iba1<sup>+</sup> cell and GFAP-LI /GFAP<sup>+</sup> cell in the hilus of the DG in three group as an index of reactive microglia and astrocyte by a densitometric analysis. Data are shown as mean with S.E.M (n=6). \* $P < 0.05$  (ANOVA followed by Tukey test). **D)** Typical profile of active caspase 3<sup>+</sup>/DCX<sup>+</sup> cells in the DG in three groups (PBS, ESM and BQ788). Coronal sections fitting to the same atlas images from each group (8 h after treatment) were immunostained with anti-active caspase 3 (green) and anti-DCX (red). All sections were stained with DAPI (blue). **E)** The number of cells coexpressing active caspase 3 and DCX in the hilus of the DG in three group. Data are shown as mean with S.E.M (n=6). \* $P < 0.05$  (ANOVA followed by Tukey test). **F)** ESM induces cerebral vascular leakage in the hippocampus. Hippocampi of coronal sections fitting to the same atlas images from the FITC-dextran-loaded brains of each group (8 h after treatment) were observed under a fluorescence microscope. The fluorescence intensity of FITC was analyzed by a densitometer. Data are shown as mean



with S.E.M (n=4). \* $P < 0.05$  (ANOVA followed by Tukey test).

**Figure 3** ESM activates neuroendocrine cells in the hypothalamic PVN. **A)** Typical profile of c-FOS<sup>+</sup> cells in the hypothalamic PVN in three groups (PBS, ESM and BQ788). Coronal sections fitting to the same atlas images from each group (8 h after treatment) were immunostained with anti-c-FOS (red). All sections were stained with DAPI (blue). **B)** The number of cells expressing c-FOS in the hypothalamic PVN in three groups. Data are shown as mean with S.E.M (n=6). \* $P < 0.05$  (ANOVA followed by Tukey test). **C)** ESM-induced c-FOS-LI is mostly localized in AVP<sup>+</sup> cells. Coronal sections from ESM group (8 h after treatment) were immunostained with c-FOS (red) and anti-AVP (green). All sections were stained with DAPI (blue). **D)** The number of cells expressing Iba1 or GFAP in the hypothalamic PVN in three groups. Data are shown as mean with S.E.M (n=6). \* $P < 0.05$  (ANOVA followed by Tukey test). **E)** ESM induces cerebral vascular leakage in the hypothalamus. Hypothalami of coronal sections fitting to the same atlas images from the FITC-dextran-loaded brains of each group (8 h after treatment) were observed under a fluorescence microscope. The fluorescence intensity of FITC was analyzed by a densitometer. Data are shown as mean with S.E.M (n=4). \* $P < 0.05$  (ANOVA followed by

Tukey test).

**Figure 4** ESM-induced proinflammatory mediators in the specific sites of brain. **A)** Typical profiles of protein array for 40 cytokines in three groups (PBS, ESM and BQ788). 13 molecules (> 200% induction, ESM vs. PBS; > 30% reduction, BQ788 vs. ESM) showing reproducible profile in two experiments were selected by a densitometric analysis and indicated with the correct location in the membrane map. **B)** Densitometric analysis of the 13 molecules in three groups. Signal intensity is expressed as arbitrary units relative to the positive internal control.

Life Sciences vol.118 No.2  
平成 26 年 3 月 20 日公表済